

# Thermal decomposition kinetics of potassium iodate

## Part I. The effect of particle size on the rate and kinetics of decomposition

K. Muraleedharan

Received: 25 April 2011 / Accepted: 26 May 2011 / Published online: 11 June 2011  
© Akadémiai Kiadó, Budapest, Hungary 2011

**Abstract** The rate and kinetics of the thermal decomposition of potassium iodate ( $\text{KIO}_3$ ) has been studied as a function of particle size, in the range 63–150  $\mu\text{m}$ , by isothermal thermogravimetry at different temperatures, 790, 795, 800 and 805 K in nitrogen atmosphere. The theoretical and experimental mass loss data are in good agreement for the thermal decomposition of all samples of  $\text{KIO}_3$  at all temperatures studied. The isothermal decomposition of all samples of  $\text{KIO}_3$  was subjected to both model-fitting and model-free (isoconversional) kinetic methods of analysis. It has been observed that the activation energy values are independent of the particle size. Isothermal model-fitting analysis shows that the thermal decomposition kinetics of all the samples of  $\text{KIO}_3$  studied can be best described by the contracting cube equation.

**Keywords** Contracting cube equation · Effect of particle size · Isothermal thermogravimetry · Potassium iodate · Kinetics and mechanism

### Introduction

Information about the thermal stability of solid materials of all kinds is of great practical and technological importance [1–3]. Thermogravimetric analysis (TG) is usually adopted to study the kinetics of thermally activated solid-state reactions to obtain thermal stability parameters of solids [4–8]. The kinetics of the thermal decomposition of inorganic materials could be markedly affected by pre-

treatments, by the shortening of the induction period followed by an overall decrease in time needed to complete the reaction. The thermal decomposition data generated from TG can be analyzed and manipulated to obtain kinetic parameters, such as activation energy ( $E$ ) and pre-exponential factor ( $A$ ) [9–11]. Solid-state kinetic data are of practical interest for the large and growing number of technologically important processes. Kinetic studies predict how quickly a system approaches equilibrium and also help to understand the mechanism of the process [12, 13]. A number of reviews are available in the literature on these processes [14–21]. Several authors have emphasized the practical and theoretical importance of information on the kinetics and mechanism of solid-state decompositions [1, 22–24].

Thermoanalytical studies showed that  $\text{KIO}_3$  decomposes with heat evolution to potassium iodide (KI) and oxygen in the temperature range 795–815 K with an overall decomposition of the type  $A \rightarrow B + C$ , where  $A$  and  $B$  are solid phases and  $C$  is a gas [25]. This type of reactions, typically resulting in highly reactive solid products, has attracted a big deal of research because of their theoretical and technical relevance.

Solymosi reported that the thermal decomposition reaction of  $\text{KIO}_3$ , at one atmosphere pressure and in the temperature range 485–520 °C, is autocatalytic and observed rapid reaction up to 25–30% conversion; beyond which the reaction suddenly slows down and show a maximum rate around 26% conversion [26]. The Prout–Tompkins [27] equation proved to be the most suitable for kinetic analysis of the decomposition curve;  $E$  values of 258 and 224  $\text{kJ mol}^{-1}$  were reported for the acceleratory and the decay period, respectively [26]. Chloride, bromide and iodide ions exerted considerable acceleratory effects on the reaction. At higher temperatures, the decomposition

K. Muraleedharan (✉)  
Department of Chemistry, University of Calicut,  
Calicut, Kerala 673 635, India  
e-mail: kmuralika@gmail.com

was found to be of deceleratory in nature; at lower temperatures, the rate maximum occurred at smaller conversions. The presence of halides decreased the activation energy of the thermal decomposition reaction. Nickel oxide effectively catalyzed the decomposition. In this case too, the decomposition started with the highest rate. The first-order equation was found to be the most suitable for the calculation of rate constant of the catalytic reaction. The value of the activation energy observed was  $216 \text{ kJ mol}^{-1}$ . Although potassium iodate decomposes on heating at 750 K, in high vacuum ( $10^{-6}$  mbar), mass spectrometric studies detected volatilization of the molecular species,  $\text{KIO}_3$  [28]. It has been found, on survey of the literature, that no more studies on the thermal decomposition and kinetics of potassium iodate are reported in the literature.

Our earlier investigations showed that the isothermal decomposition of  $\text{KIO}_3$  proceeds through contracting cube model kinetics with activation energy value around  $336 \text{ kJ mol}^{-1}$ , at all temperatures studied [25]. The objective of this work is to investigate the effect of particle size on the thermal decomposition kinetics of  $\text{KIO}_3$  by isothermal thermogravimetry. In this study, the influence of heat and mass transfer phenomena has been left aside. The great emphasis is given to reliable activation energy values for the forward reaction,  $2\text{KIO}_3 \rightarrow 2\text{KI} + \text{O}_2$ , which allows one to draw mechanistic conclusions as well as to predict the kinetics of the process.

## Experimental

AnalaR grade  $\text{KIO}_3$  of E Merck is dissolved in water, recrystallized, dried and kept in vacuum desiccator. To study the effect of *particle size*, recrystallized  $\text{KIO}_3$  sample was powdered in an agate mortar, sieved into five different particle size ranges, such as 63–75, 75–90, 90–106, 106–125 and 125–150  $\mu\text{m}$  and kept in a vacuum desiccator. The isothermal analyses of  $\text{KIO}_3$  samples were carried out on a T. A. thermal analyzer, model: TGA Q50 V20.2 Build 27 at four different temperatures, such as 790, 795, 800 and 805 K. The operational characteristics of the thermal analyzer system are atmosphere: flowing nitrogen, at a flow rate of  $6 \times 10^{-2} \text{ L min}^{-1}$ ; sample mass: 10 mg; sample pan: silica. Duplicate run was made under similar conditions and found that the data overlap with each other, indicating satisfactory reproducibility.

## Results and discussion

The isothermal TG curves for  $\text{KIO}_3$  sample having a particle size of 90–106  $\mu\text{m}$ , at different temperatures, in nitrogen atmosphere were reported earlier [25]. Similar

curves were obtained for the thermal decomposition of all other samples of  $\text{KIO}_3$  studied (not shown).

### Calculation of fractional decomposition, $\alpha$

On the assumption that both solid and gaseous products maintain a constant composition, the conventional dimensionless *fractional decomposition*,  $\alpha$ , at any time during the thermal decomposition is measured directly from the mass loss at that time relative to the overall mass loss when decomposition is complete. Thus, the TG mass loss data are transformed into  $\alpha$  using the following relation:

$$\alpha = \frac{(m_0 - m_t)}{(m_0 - m_f)},$$

where  $m_0$  is the initial mass of reactant,  $m_t$  is the mass of the reactant at time,  $t$  and  $m_f$  are the mass of the residue at infinite time.

The experimental mass loss data obtained from TG were transformed into  $\alpha - t$  data, in the range  $\alpha = 0.05 - 0.95$  with an interval of 0.05, for all the samples studied. The  $\alpha - t$  curves for the isothermal decomposition of  $\text{KIO}_3$  sample having a particle size of 90–106  $\mu\text{m}$ , at different temperatures, have been already reported [25]. Similar types of curves were obtained for the isothermal decomposition of all other samples of  $\text{KIO}_3$  studied and are shown in Fig. 1. The observed mass changes for the decomposition agree very well with the theoretical value for all samples of  $\text{KIO}_3$  at all temperatures studied.

### Model-fitting method

The  $\alpha - t$  data in the range  $\alpha = 0.05 - 0.95$  of the isothermal decomposition of all samples of  $\text{KIO}_3$  were subjected to weighted least squares analysis to various kinetic (reaction) models [25]. Typical model-fitting plots for various kinetic models for the thermal decomposition of  $\text{KIO}_3$  (particle size: 90–106  $\mu\text{m}$ ) in the range  $\alpha = 0.05 - 0.95$  at 790 K are shown in Figs. 2, 3, 4 and 5. Similar fits were obtained at all other temperatures studied (not shown). The values of slope and correlation coefficient ( $r$ ) obtained by weighted least squares plot for the isothermal decomposition of  $\text{KIO}_3$  (particle size: 90–106  $\mu\text{m}$ ) at 790, 795, 800 and 805 K for all kinetic models studied are given in Table 2. Perusal of Table 1 and Figs. 2, 3, 4 and 5 shows that the contracting cube equation,  $1 - (1 - \alpha)^{1/3} = kt$ , gave the best fits ( $r = 0.9999$ ) at all temperatures studied. Similar results were obtained for all other samples and at all temperatures studied. Figure 6 shows typical weighted least squares fits, at 790 K for contracting cube model, for all the samples of  $\text{KIO}_3$  studied.

**Fig. 1**  $\alpha - t$  plots for the isothermal decomposition of  $\text{KIO}_3$  at different temperatures and particle size ranges: **a** 63–75, **b** 75–90, **c** 106–125 and **d** 125–150  $\mu\text{m}$

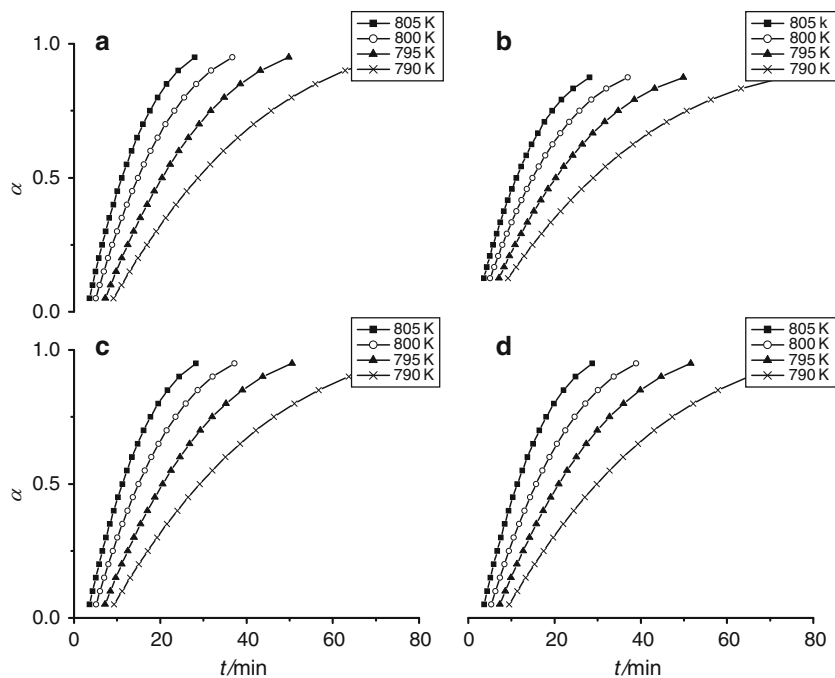
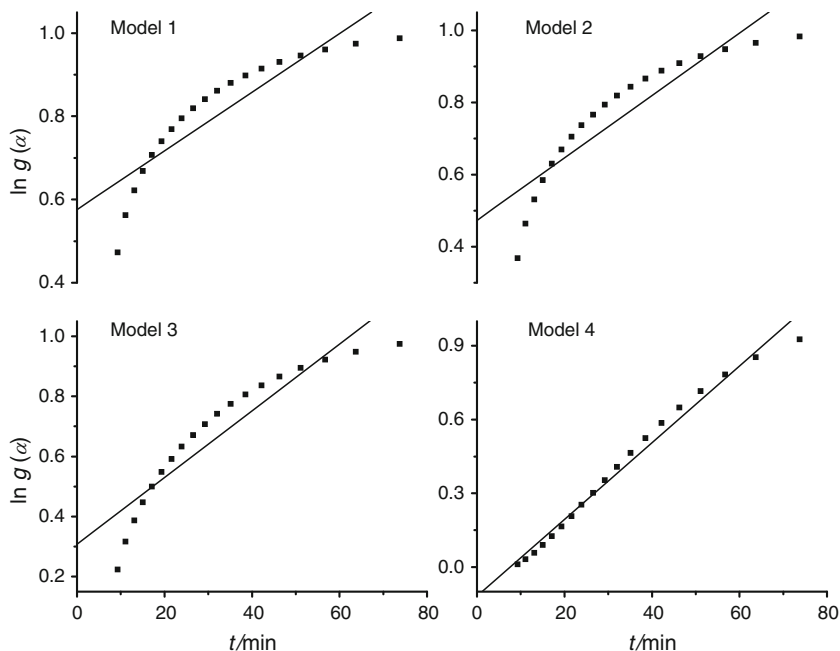


**Fig. 2** Isothermal decomposition of  $\text{KIO}_3$  at 790 K: typical model fits for Models 1–4



The effect of particle size on the thermal decomposition of  $\text{KIO}_3$  is shown in Table 2 and Fig. 7. The rate is strongly dependent on particle size; it increases as the particle size decreases. The Arrhenius plots for the isothermal decomposition of all the samples of  $\text{KIO}_3$  are shown in Fig. 8. Values of  $E$  and  $r$  are also shown in Fig. 8. This investigation showed that the  $E$  values obtained, from contracting cube model, for all the samples of  $\text{KIO}_3$  studied remain within  $336.7 \pm 1.8 \text{ kJ mol}^{-1}$ .

#### Model-free method

Model-free kinetics rests on evaluating the  $E_\alpha$  dependence that is adequate for both theoretical and practical purposes of kinetic predictions [29]. Normally, model-free kinetics does not concern with evaluating  $A$  and  $g(\alpha)$  or  $f(\alpha)$  because they are not needed for performing kinetic predictions. Also, these values are hardly suitable for theoretical interpretation because of the strong ambiguity associated

**Fig. 3** Isothermal decomposition of  $\text{KIO}_3$  at 790 K: typical model fits for Models 5–8

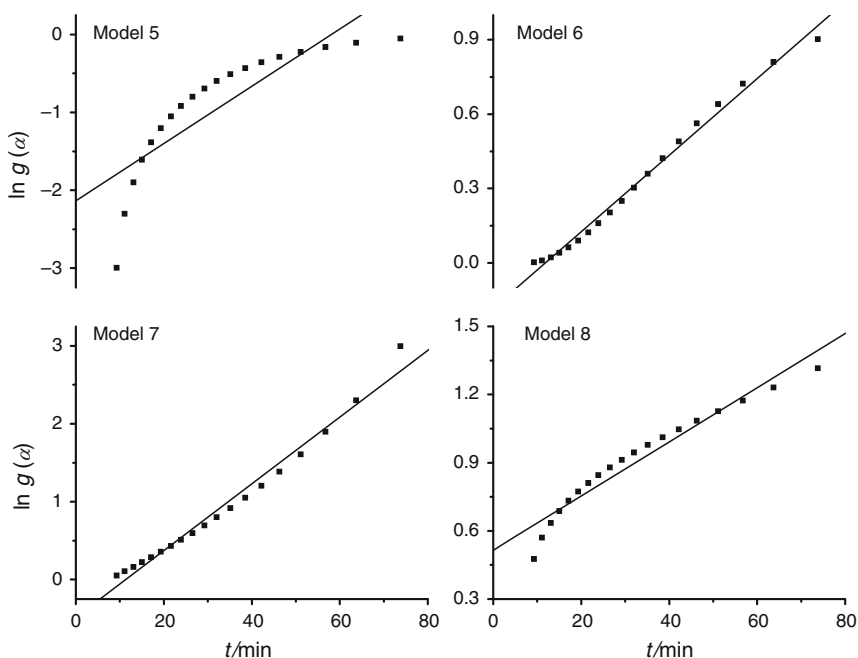
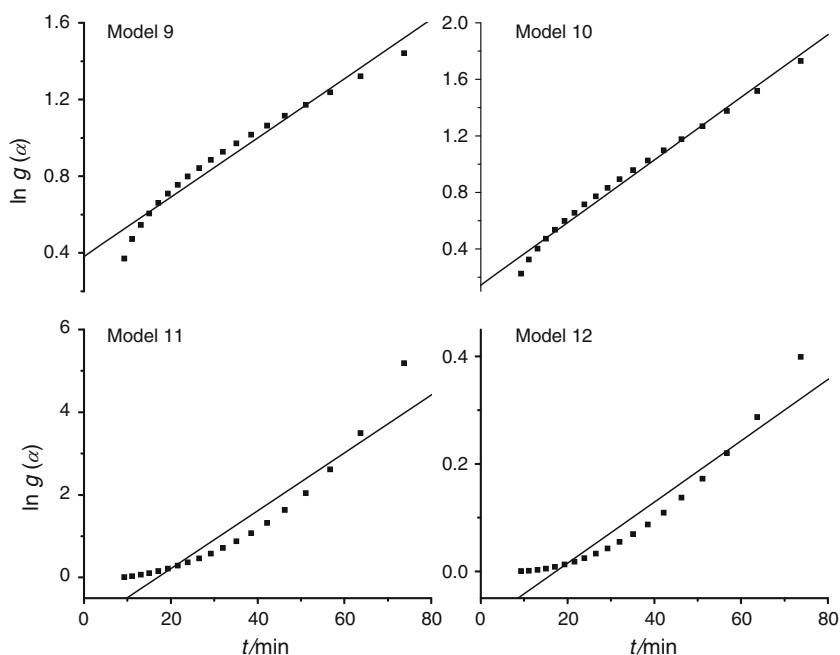


**Fig. 4** Isothermal decomposition of  $\text{KIO}_3$  at 790 K: typical model fits for Models 9–12



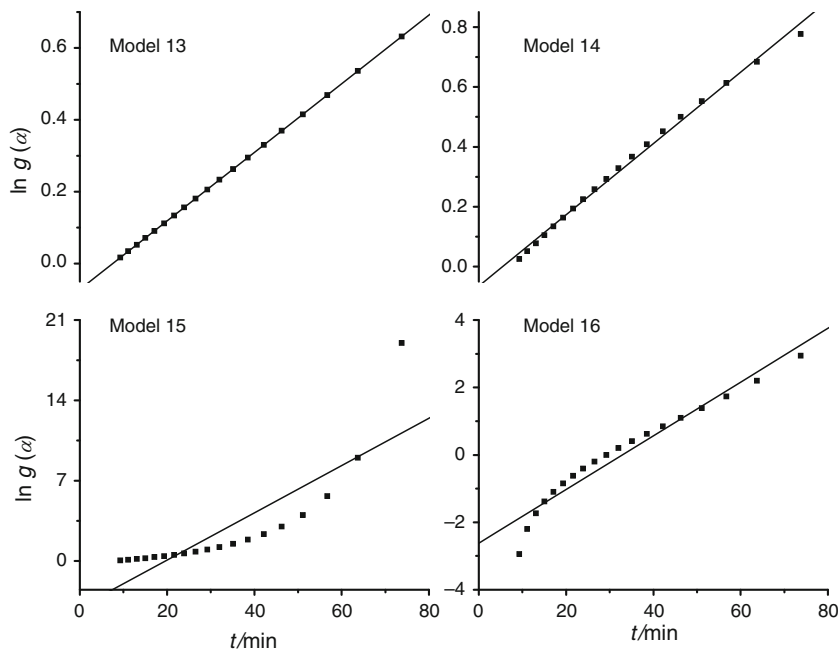
with them. However, these values can be determined in the frameworks of model-free kinetics.

The  $\alpha - t$  data, in the range of  $\alpha = 0.05$ – $0.95$ , of the isothermal decomposition of  $\text{KIO}_3$  were also subjected to isoconversional studies for the determination of apparent activation energy as a function of  $\alpha$  from the sets of isothermals obtained. A plot of  $\ln t$  ( $t$  being the time required for reaching a given value of  $\alpha$  at a constant temperature  $T$ ) versus the corresponding reciprocal of the temperature ( $1/T$ ) leads to the activation energy for the given value of  $\alpha$ . Typical isoconversional plots for the isothermal

decomposition of  $\text{KIO}_3$  (particle size:  $106$ – $125 \mu\text{m}$ ) are shown in Fig. 9. Similar plots were obtained for all other samples and at all conversions studied (not shown). The results are given in Table 3 and also shown in Fig. 10. A perusal of Table 3 reveals that the  $E$  values of all samples and at all conversions lie in the range,  $335$ – $338 \text{ kJ mol}^{-1}$ , which is in good agreement with those obtained from conventional method.

The high values of activation energy values observed in this study are generally characteristic of the decomposition reactions of metal oxy halides. The initial step in the

**Fig. 5** Isothermal decomposition of  $\text{KIO}_3$  at 790 K: typical model fits for Models 13–16



thermal decomposition is the rupture of an I–O bond, and the energy barrier to the reactions is not very sensitive to the properties of the cation present [1].

The results presented in Table 2 show that the rate constant increases with decrease in the particle size (i.e., with an increase in the surface area). This behaviour is shown in Fig. 8 where the rate of reaction is plotted against the average particle size of the grains, calculated

according to the Andreasen method [30]. A similar effect has been reported in the thermal decomposition of  $\text{NaN}_3$  [31] and in the thermal decomposition [32] and sublimation [33] of ammonium perchlorate. It has been shown by several authors that particle size is an important factor in the kinetics of the thermal decomposition of solids [31, 32, 34–37]. Huang et al. [38] have studied the effect of particle size on combustion of aluminium particle dust in

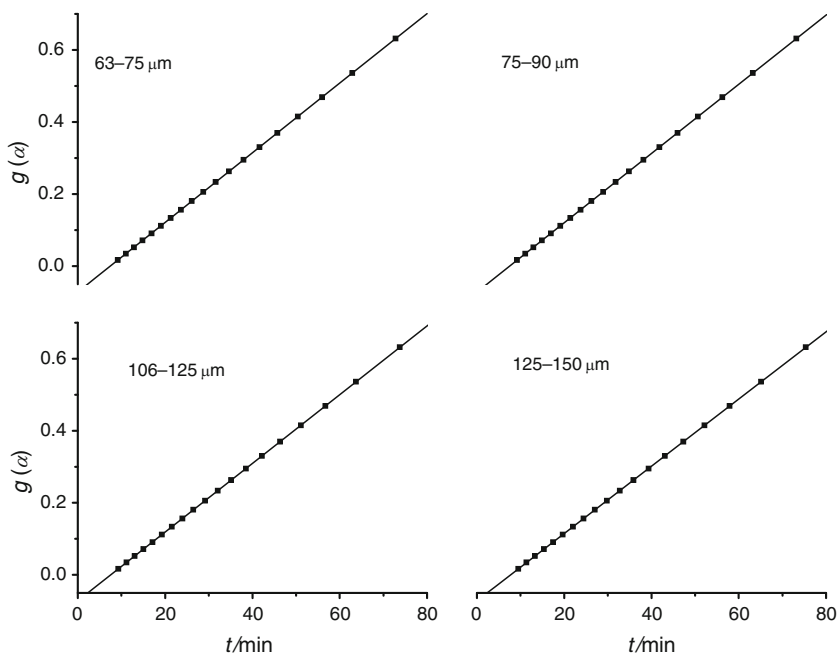
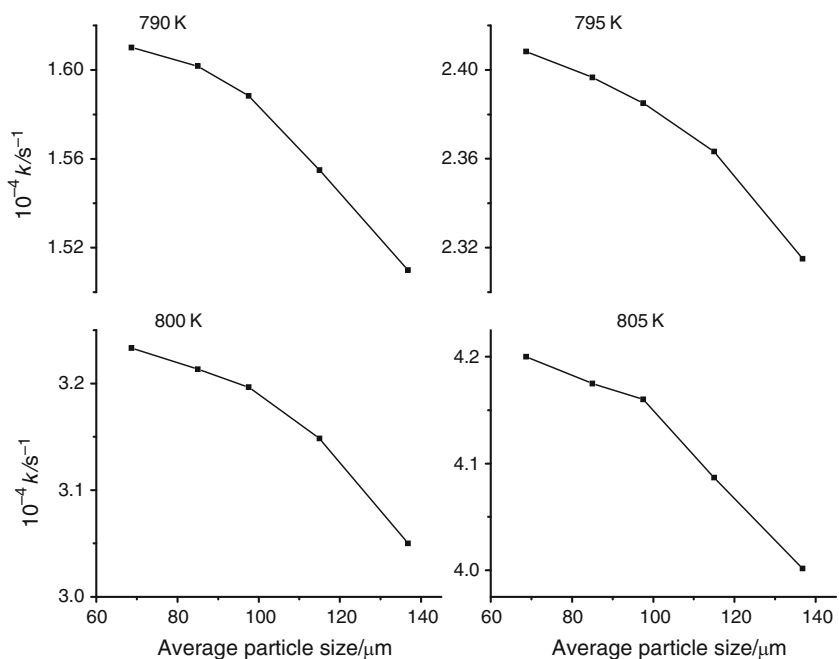
**Table 1** Values of slope, correlation coefficient ( $r$ ) obtained from isothermal model fitting to various kinetic equations at different temperatures

Model no.	Temperature/K							
	790		795		800		805	
	Slope/ $\text{min}^{-1}$	$r$	Slope/ $\text{min}^{-1}$	$r$	Slope/ $\text{min}^{-1}$	$r$	Slope/ $\text{min}^{-1}$	$r$
1	0.0070	0.8946	0.0106	0.8946	0.0142	0.8947	0.0185	0.8950
2	0.0087	0.9074	0.0130	0.9075	0.0174	0.9075	0.0227	0.9079
3	0.0111	0.9298	0.0167	0.9298	0.0223	0.9298	0.0291	0.9302
4	0.0156	0.9919	0.0234	0.9918	0.0314	0.9920	0.0408	0.9920
5	0.0368	0.8492	0.055	0.8493	0.0740	0.8493	0.0963	0.8497
6	0.0155	0.9959	0.0232	0.9959	0.0311	0.9960	0.0405	0.9959
7	0.0429	0.9902	0.0644	0.9902	0.0862	0.9901	0.1122	0.9900
8	0.0119	0.9707	0.0179	0.9708	0.0240	0.9708	0.0312	0.9710
9	0.0154	0.9811	0.0232	0.9809	0.0311	0.9809	0.0404	0.9811
10	0.0225	0.9942	0.0333	0.9942	0.0446	0.9942	0.0580	0.9943
11	0.0701	0.9501	0.1052	0.9502	0.1410	0.9498	0.1834	0.9497
12	0.0057	0.9593	0.0086	0.9594	0.0115	0.9590	0.0149	0.9590
13	0.0095	<i>0.9999</i>	0.0143	<i>0.9999</i>	0.0192	<i>0.9999</i>	0.0250	<i>0.9999</i>
14	0.0119	0.9979	0.0179	0.9979	0.0240	0.9979	0.0312	0.9980
15	0.2062	0.8455	0.3097	0.8457	0.4146	0.8448	0.5395	0.8448
16	0.0796	0.9737	0.1196	0.9738	0.1602	0.9737	0.2085	0.9739

Italics values indicate the maximum correlation coefficient

**Table 2** The effect of particle size on the rate of isothermal decomposition of  $\text{KIO}_3$  at different temperatures

Particle size range/ $\mu\text{m}$	Average particle size/ $\mu\text{m}$	$k \times 10^{-4}/\text{s}^{-1}$			
		790 K	795 K	800 K	805 K
63–75	68.65	1.6100	2.4083	3.2333	4.2000
75–90	85.04	1.6017	2.3967	3.2133	4.1750
90–106	97.56	1.5883	2.3850	3.1967	4.1600
106–125	114.98	1.5550	2.3633	3.1483	4.0867
125–150	136.74	1.5100	2.3150	3.0500	4.0017

**Fig. 6** The thermal decomposition of  $\text{KIO}_3$  samples at 790 K: Least squares fit, for contacting cube model, of the  $g(x) - t$  data of samples having different particle size ranges**Fig. 7** Effect of particle size on the rate of the isothermal decomposition of  $\text{KIO}_3$  at different temperatures

**Fig. 8** Arrhenius plots for the isothermal decomposition of  $\text{KIO}_3$ . Particle size: **a** 63–75, **b** 75–90, **c** 106–125 and **d** 125–150  $\mu\text{m}$

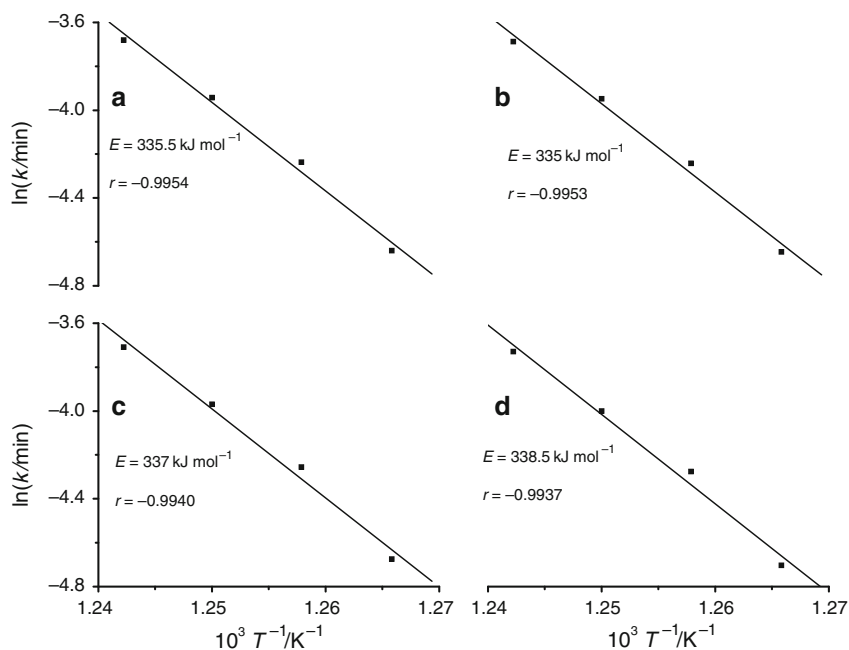
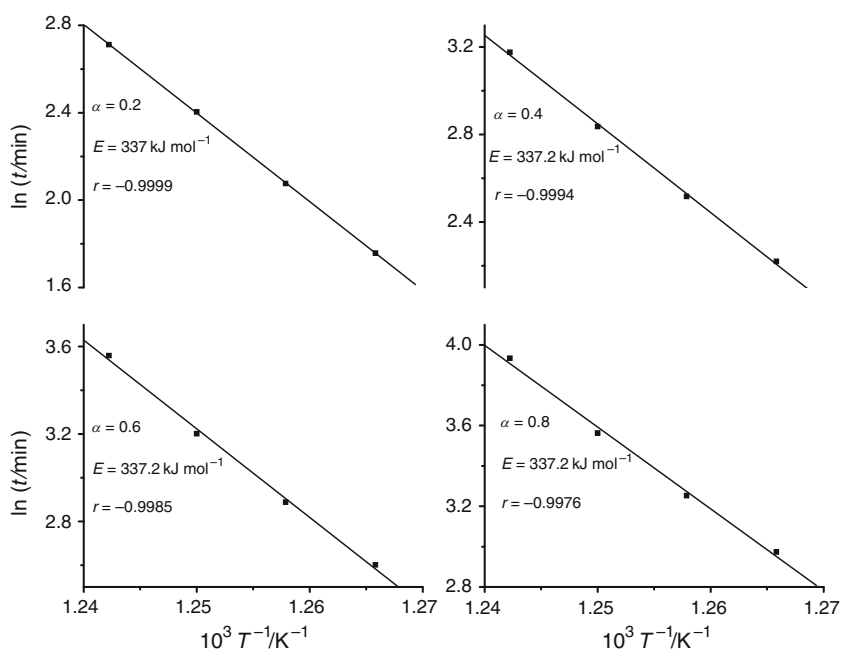


**Fig. 9** Typical isoconversional plots for the thermal decomposition of  $\text{KIO}_3$  (particle size: 106–125  $\mu\text{m}$ )

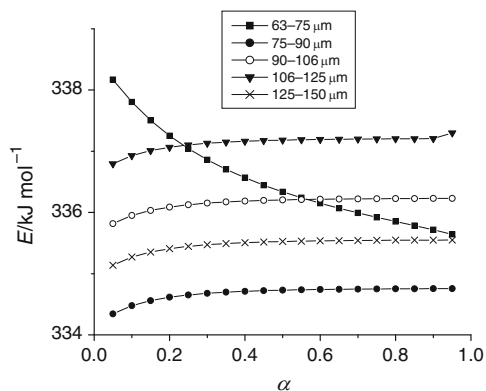


air and observed that the particle burning time is size dependent. Chou and Olsen [39] found an unusual dependence of rate on particle size in the thermal decomposition of isothiocyanatopentaammine cobalt(III) perchlorate. They observed that when  $\alpha$  was less than 0.09, the larger particles decomposed relatively rapidly with an activation energy value of  $138 \text{ kJ mol}^{-1}$  and thereafter the reaction rate decreased and the decomposition proceeds with activation energy values in between 88 and  $117 \text{ kJ mol}^{-1}$ .

It is well known that the gross imperfections are present more on the surface than in the bulk [33]. When the particle size is decreased, the surface area increases that in turn results in an increase in the concentration of gross imperfections. The larger the concentration of gross imperfections, the greater the number of nuclei formed [32] leading to an enhancement in the rate of decomposition. The thermal decomposition of solids in which the rate increases by decreasing the particle size [32] has been explained on the basis of Mampel's theory.

**Table 3** Values of  $E$  and correlation coefficient ( $r$ ) obtained from isothermal isoconversional analysis at different particle size ranges

Particle size/ $\mu\text{m}$	63–75		75–90		90–106		106–125		125–150	
	$E/\text{kJ mol}^{-1}$	$-r$	$E/\text{kJ mol}^{-1}$	$-r$	$E/\text{kJ mol}^{-1}$	$-r$	$E/\text{kJ mol}^{-1}$	$-r$	$E/\text{kJ mol}^{-1}$	$-r$
0.05	338.2	0.9958	334.3	0.9983	335.8	0.9984	336.8	0.9979	335.1	0.9967
0.1	337.8	0.9980	334.5	0.9995	336.0	0.9995	336.9	0.9992	335.3	0.9984
0.15	337.5	0.9991	334.6	0.9999	336.0	0.9999	337.0	0.9998	335.4	0.9993
0.2	337.3	0.9997	334.6	1.0000	336.1	1.0000	337.1	1.0000	335.4	0.9996
0.25	337.0	0.9998	334.7	0.9999	336.1	0.9999	337.1	0.9999	335.4	0.9998
0.3	336.9	0.9998	334.7	-0.9997	336.2	0.9997	337.1	0.9998	335.5	0.9998
0.35	336.7	0.9997	334.7	0.9994	336.2	0.9994	337.1	0.9996	335.5	0.9997
0.4	336.6	0.9995	334.7	0.9992	336.2	0.9991	337.2	0.9994	335.5	0.9996
0.45	336.4	0.9993	334.7	0.9989	336.2	0.9988	337.2	0.9992	335.5	0.9994
0.5	336.3	0.9991	334.7	0.9986	336.2	0.9985	337.2	0.9989	335.5	0.9992
0.55	336.2	0.9988	334.7	0.9984	336.2	0.9983	337.2	0.9987	335.5	0.9991
0.6	336.2	0.9986	334.7	0.9981	336.2	0.9980	337.2	0.9985	335.5	0.9989
0.65	336.1	0.9983	334.7	0.9978	336.2	0.9978	337.2	0.9983	335.5	0.9987
0.7	336.0	0.9981	334.7	0.9976	336.2	0.9975	337.2	0.9980	335.5	0.9985
0.75	335.9	0.9978	334.8	0.9974	336.2	0.9973	337.2	0.9978	335.5	0.9984
0.8	335.9	0.9976	334.8	0.9971	336.2	0.9970	337.2	0.9976	335.5	0.9982
0.85	335.8	0.9973	334.8	0.9969	336.2	0.9968	337.2	0.9974	335.5	0.9980
0.9	335.7	0.9970	334.8	0.9966	336.2	0.9965	337.2	0.9972	335.5	0.9978
0.95	335.6	0.9967	334.8	0.9963	336.2	0.9962	337.3	0.9974	335.5	0.9976

**Fig. 10** Plots of  $E$  versus conversion for all samples of  $\text{KIO}_3$ 

Mampel's theory is concerned with nucleation and growth in systems consisting of microcrystals in the form of spheres, and theoretically, Mampel has shown that the isothermal decomposition rate of a solid should increase because, as the particle size is decreased (i.e., when the surface area is increased), the number of surface defects, which can act as potential nucleus-forming sites, increases leading to an enhanced nucleation and growth, or in other words, a sensitization in the rate of decomposition.

## Conclusions

The importance of surface in solid-state reactions is illustrated in the study of the decomposition reaction as a function of particle size. This study showed that in the isothermal decomposition of  $\text{KIO}_3$ , the rate increases as the particle size decreases; the mechanism of the reaction, contracting cube equation, remains the same. Furthermore, the thermal decomposition reaction shows consistent values of  $E$  for the entire range of particle size studied. The surface area increases with decrease in particle size; consequently, the number of the "germ nuclei" also increases leading to an increase in rate.

The rate of solid-state reactions is usually controlled either by *electron transfer* or *diffusion* (of ions in the lattice) mechanism. Electron transfer mechanism involves the transfer of an electron from the iodate anion to potassium cation to form the free radicals  $\text{K}^\bullet$  and  $\text{IO}_3^\bullet$ . As  $\text{IO}_3^\bullet$  involves a one-electron bond, it is very unstable and readily decomposes to give  $\text{O}^\bullet$  and relatively stable  $\text{I}^\bullet$ . Two  $\text{O}^\bullet$  species combine to give one oxygen molecule.  $\text{I}^\bullet$  is stabilized by receiving an electron from  $\text{K}^\bullet$  forming  $\text{KI}$ . In the case of diffusion mechanism, the rate may be controlled by the diffusive escape of the volatile product, oxygen. Further investigations, such as pretreatment studies, are required to clearly establish the mechanism, the rate-determining step, of the thermal decomposition of  $\text{KIO}_3$ .



This work demonstrates how strongly the particle size of the sample influences the reactivity of  $\text{KIO}_3$  providing information to the solid-state reactivity database.

## References

- Galwey AK, Brown ME. Thermal decomposition of ionic solids. Amsterdam: Elsevier; 1999.
- Stern KH. High temperature properties and thermal decomposition of inorganic salts with oxy anions. Florida: CRC; 2001.
- Vyazovkin S. Thermal analysis. *Anal Chem.* 2004;76:3299–312.
- Deng C, Cai J, Liu R. Kinetic analysis of solid state reactions: evaluation of approximations to temperature integral and their applications. *Solid State Sci.* 2009;11:1375–9.
- Vecchio S, Rodante F, Tomassetti M. Thermal stability of disodium and calcium phosphomycin and the effects of the excipients evaluated by thermal analysis. *J Pharm Biomed Anal.* 2001;24:1111–23.
- Huang Y, Cheng Y, Alexander K, Dollimore D. The thermal analysis study of the drug captopril. *Thermochim Acta.* 2001;367:43–58.
- Dollimore D, O'Connell C. A comparison of the thermal decomposition of preservatives, using thermogravimetry and rising temperature kinetics. *Thermochim Acta.* 1998;324:33–48.
- Halikia I, Neou-Syngouna P, Kolitsa D. Isothermal kinetic analysis of the thermal decomposition of magnesium hydroxide using thermogravimetric data. *Thermochim Acta.* 1998;320:75–88.
- Vyazovkin S, Wight CA. Model-free and model-fitting approaches to kinetic analysis of isothermal and nonisothermal data. *Thermochim Acta.* 1999;340–341:53–68.
- Rodante F, Vecchio S, Tomassetti M. Kinetic analysis of thermal decomposition for penicillin sodium salts: model-fitting and model-free methods. *J Pharm Biomed Anal.* 2002;29:1031–43.
- Brown ME. Introduction to thermal analysis: techniques and applications. 2nd ed. The Netherlands: Kluwer; 2001.
- Malek J, Mitsuhashi T, Criado JM. Kinetic analysis of solid-state processes. *J Mater Res.* 2001;16:1862–71.
- Zhou D, Schmitt EA, Zhang GG, Law D, Vyazovkin S, Wight CA, Grant DJW. Crystallization kinetics of amorphous nifedipine studied by model-fitting and model-free approaches. *J Pharmaceutical Sci.* 2003;92:1779–91.
- Benderskii VA, Makarov DE, Wight CA. Chemical dynamics at low temperatures. New York: Wiley; 1994. p. 385.
- Brown ME, Dollimore D, Galwey AK. Reactions in the solid state, comprehensive chemical kinetics, Vol. 22. Amsterdam: Elsevier; 1980. pp 340.
- Vyazovkin S, Wight CA. Isothermal and nonisothermal reaction kinetics in solids: in search of ways toward consensus. *J Phys Chem.* 1997;101A:8279–84.
- Brill TB, James KJ. Kinetics and mechanisms of thermal decomposition of nitroaromatic explosives. *Chem Rev.* 1993;93:2667–92.
- Mark HF, Bikales NM, Overberger CG, Menges G, editors. Encyclopedia of polymer science and engineering. New York: Wiley; 1989. p. 231–690.
- Vyazovkin S, Wight CA. Isothermal and nonisothermal kinetics of thermally stimulated reactions of solids. *Int Rev Phys Chem.* 1998;17:407–33.
- Dollimore D. Thermal analysis. *Chem Rev.* 1996;68:63–72.
- Galwey AK. Is the science of thermal analysis kinetics based on solid foundations? A literature appraisal. *Thermochim Acta.* 2004;413:139–83.
- Vyazovkin S. Kinetic concepts of thermally stimulated reactions in solids: a view from a historical perspective. *Int Rev Phys Chem.* 2000;19:45–60.
- Kotler JM, Hinman NW, Richardson CD, Scott JR. *J Thermal Anal Calorim.* 2010;102:23–9.
- Bertol CD, Cruz AP, Stulzer HK, Murakami FS, Silva MAS. Thermal decomposition behaviour of potassium and sodium jasorite synthesized in the presence of methyl amine and alanine. *J Thermal Anal Calorim.* 2010;102:187–92.
- Muraleedharan K, Kannan MP, Ganga Devi T. Thermal decomposition kinetics of potassium iodate. *J Thermal Anal Calorim.* 2011;103:943–55.
- Solymosi F. Structure and stability of salts of halogen oxyacids in the solid phase. London: Wiley; 1977.
- Prout EG, Tompkins FC. The thermal decomposition of potassium permanganate. *Trans Faraday Soc.* 1944;40:488–97.
- Bhatta D, Padhee G. Role of  $\gamma$ -irradiation and  $\text{Ba}^{2+}$  doping on the isothermal decomposition of caesium bromate. *J Thermal Anal Calorim.* 1991;37:2693–9.
- Vyazovkin S. Model-free kinetics staying free of multiplying entities without necessity. *J Thermal Anal Calorim.* 2006;83:45–51.
- Kenneth Shaw, editor. Principles of solid-state chemistry. Reactions in solids. London: MacLaren; 1968. p. 21.
- Nakamura H, Sakumoto K, Hara Y, Ochi K. Thermal analysis of sodium azide. *J Hazard Mat.* 1994;38:1–12.
- Bircumshaw LL, Newman BH. The thermal decomposition of ammonium perchlorate. II. The kinetics of the decomposition, the effect of particle size, and discussion of results. *Proc Roy Soc Lond.* 1955;A227:228–41.
- Pai Verneker VR, Kishore K, Kannan MP. Effect of pretreatment on the sublimation of ammonium perchlorate. *J Appl Chem Biotechnol.* 1977;27:309–17.
- Maycock JN, Pai Verneker VR, Rouch L Jr. Influence of growth parameters on the reactivity of ammonium perchlorate. *Inorg Nuc Chem Lett.* 1968;4:119–23.
- Boldyrev VV, Avvakumov L. Mechanochemistry of inorganic solids. *Russ Chem Rev.* 1971;40:847–59.
- Pai Verneker VR, Maycock JN. The thermal decomposition of ammonium perchlorate at low temperature. *J Inorg Nucl Chem.* 1967;29:2723–30.
- Mitchell JW, DeVries RC, Roberts RW, Cynon P, editors. Reactivity of solids. New York: Wiley; 1969. p. 287.
- Huang Y, Risha GA, Yang V, Yetter RA. Effect of particle size on combustion of aluminum particle dust in air. *Combust Flame.* 2009;156:5–13.
- Chou CJ, Olsen FA. Isothermal decomposition of isothiocyanatopentaamine cobalt(III) perchlorate. Particle size effect. *Anal Chem.* 1972;44:1841–4.